

This article was downloaded by: [Victor Kovtunenکو]

On: 01 August 2012, At: 07:33

Publisher: Taylor & Francis

Informa Ltd Registered in England and Wales Registered Number: 1072954 Registered office: Mortimer House, 37-41 Mortimer Street, London W1T 3JH, UK



## Optimization: A Journal of Mathematical Programming and Operations Research

Publication details, including instructions for authors and subscription information:

<http://www.tandfonline.com/loi/gopt20>

### A hemivariational inequality in crack problems

V.A. Kovtunenکو <sup>a b</sup>

<sup>a</sup> Department of Mathematics and Scientific Computing, University of Graz, 8010 Graz, Austria

<sup>b</sup> Lavrent'ev Institute of Hydrodynamics, 630090 Novosibirsk, Russia

Version of record first published: 11 Jul 2011

To cite this article: V.A. Kovtunenکو (2011): A hemivariational inequality in crack problems, Optimization: A Journal of Mathematical Programming and Operations Research, 60:8-9, 1071-1089

To link to this article: <http://dx.doi.org/10.1080/02331934.2010.534477>

PLEASE SCROLL DOWN FOR ARTICLE

Full terms and conditions of use: <http://www.tandfonline.com/page/terms-and-conditions>

This article may be used for research, teaching, and private study purposes. Any substantial or systematic reproduction, redistribution, reselling, loan, sub-licensing, systematic supply, or distribution in any form to anyone is expressly forbidden.

The publisher does not give any warranty express or implied or make any representation that the contents will be complete or accurate or up to date. The accuracy of any instructions, formulae, and drug doses should be independently verified with primary sources. The publisher shall not be liable for any loss, actions, claims, proceedings, demand, or costs or damages whatsoever or howsoever caused arising directly or indirectly in connection with or arising out of the use of this material.

## A hemivariational inequality in crack problems

V.A. Kovtunenکو<sup>ab\*</sup>

<sup>a</sup>Department of Mathematics and Scientific Computing, University of Graz, 8010 Graz, Austria; <sup>b</sup>Lavrent'ev Institute of Hydrodynamics, 630090 Novosibirsk, Russia

(Received 15 October 2009; final version received 16 October 2010)

Interface crack problems arising in quasibrittle fracture due to contact with cohesion or plasticity between the crack faces are considered. These problems are described by a hemivariational inequality. Its solvability is guaranteed by the variational principle, which yields minimization of a nonconvex and nondifferentiable objective functional associated to the total potential energy. To compute solutions of the hemivariational inequality, a primal-dual active-set algorithm is suggested, which obeys global and monotone convergence properties. A numerical example of the quasibrittle fracture is presented.

**Keywords:** hemivariational inequality; nonconvex and nonsmooth optimization; primal-dual methods; active-set algorithm; crack problem; quasibrittle fracture

**AMS Subject Classifications:** 49J40; 49M29; 74R20; 90C90

### 1. Introduction

We consider a class of crack problems based on the physical models of Cherepanov, Barenblatt, Dugdale, Leonov–Panasyuk and Novozhilov, which describe quasibrittle fracture. The principal feature is that these models admit contact with cohesion or plasticity between the crack faces. In contrast, the classic linearized model of Griffith describing brittle fracture ignores the interaction phenomena. For the physical foundations we refer to [3,17,19,22]. Utilizing the variational approach [13] to crack problems, earlier we stated a variational principle for the cohesion problems in [15]. The optimization approach to cracks under quasibrittle fracture was suggested in [16]. In this article we aim at computational tools.

From a viewpoint of physics, the cohesion models account for the irreversible work of plastic deformations, which is caused by the normal opening of a crack. This phenomenon is relevant to a frictional interaction between the crack faces. In comparison, models of friction, adopted in contact mechanics, describe dissipation of the energy due to the tangential shear between the surfaces being in contact. For the problems of frictional cracks we refer to [12] and the references therein.

---

\*Email: kovtunenکو@uni-graz.at

To our best knowledge, there is no available mathematical model coupling both the interaction phenomena of cohesion and friction.

From an optimization point of view, the quasibrittle cracks are described by a hemivariational inequality. For the conception of hemivariational inequalities we refer to [1,5,6,23]. Their solvability is provided commonly by a constrained minimization of nonconvex and nondifferentiable objective functionals (superpotentials). For the abstract concepts of nonsmooth optimization in continuous and numerical frameworks, see [2,14,21,24,25].

In our case, the objective associates to the total potential energy subject to unilateral conditions of contact. The principal difficulty of its investigation is connected with the absence of an optimality condition, which would be simultaneously necessary and sufficient for finding a solution. In fact, the sufficient optimality condition is expressed by a minimax (saddle-point) problem. The necessary optimality condition yields a hemivariational inequality. However, the latter may obey a multiple solution which is not a minimizer of the superpotential.

To treat the hemivariational inequality numerically, we are motivated by the following observations.

In numerical optimization, generalized (semismooth) Newton methods, which are locally of the almost second order, are an efficient tool for computing of convex minimization problems. Moreover, for regular problems, semismooth Newton methods are equivalent to primal-dual active-set (PDAS) methods (see the related works by [7,11]). In the context of crack problems, these methods were developed in [8,9] and other works by the authors. However, the difficulty of the present problem concerns the absence of the generalized differentiability property of the objective function. As a consequence, the semismooth Newton method cannot be applied here directly.

To calculate a solution of the hemivariational inequality under consideration, we suggest a primal-dual setting of the problem. This formulation treats the displacement and the interaction forces (due to contact and cohesion) as independent primal and dual variables, respectively. Applying a semi-Newton method to the primal-dual form of the hemivariational inequality we arrive at a PDAS-type algorithm. The key result is that the PDAS-algorithm obeys global and monotone convergence properties like in the convex case. For more relations between PDAS methods and semismooth Newton methods applied to regularized nonconvex problems see [10].

The structure of this article is as follows. In Section 2 we model quasibrittle cracks as a hemivariational inequality. In Section 3 we derive the primal-dual setting of the crack problem. Section 4 is devoted to the PDAS-algorithm. Finally, in Section 5 we present an illustrative example of quasibrittle fracture. The numerical example is calculated using the PDAS-algorithm incorporated into an adaptive finite-element method. Its global and monotone convergence properties are justified numerically. Section 6 concludes this article.

## 2. Modelling of the crack problem

We start with the modelling of quasibrittle cracks.

Let  $\Omega \in \mathbb{R}^d$ ,  $d=2, 3$ , be a bounded domain with the (Lipschitz)  $C^{0,1}$ -boundary  $\partial\Omega$  consisting two disjoint parts  $\Gamma_N$  and  $\Gamma_D \neq \emptyset$ , and  $n=(n_1, \dots, n_d)$  be the outward normal vector to  $\partial\Omega$ . We assume that  $\Sigma$  is a  $C^{1,1}$ -surface of the Hausdorff dimension  $d-1$  such that it admits a smooth closed extension into  $\Omega$ . By  $\Sigma$  we mind *a-priori* given interface where an incipient (multi-) crack can occur. We define a normal  $v=(v_1, \dots, v_d)$  and a tangential  $\tau=(\tau_1, \dots, \tau_d)$  vectors at  $\Sigma$ . Let the direction of  $\pm v$  distinguish the positive  $\Sigma^+$  and the negative  $\Sigma^-$  faces of  $\Sigma$ , respectively. We denote with  $\Omega_\Sigma = \Omega \setminus \overline{\Sigma}$ , the domain bounded by the outer boundary  $\partial\Omega = \Gamma_N \cup \Gamma_D$  and the surfaces  $\Sigma^\pm$ .

For the displacement  $u=(u_1, \dots, u_d)(x)$  of points  $x=(x_1, \dots, x_d)$  in  $\Omega_\Sigma$ , we introduce the standard linear stress and strain tensors

$$\begin{aligned} \sigma_{ij}(u) &= c_{ijkl}\varepsilon_{kl}(u), \quad \varepsilon_{ij}(u) = \frac{1}{2}(u_{i,j} + u_{j,i}), \quad i, j = 1, \dots, d, \\ 0 < c_0 &\leq c_1 < \infty, \quad c_0\xi_{ij}\xi_{ij} \leq c_{ijkl}(x)\xi_{kl}\xi_{ij} \leq c_1\xi_{ij}\xi_{ij} \\ &\text{for all } x \in \Omega_\Sigma \text{ and } \xi \in \mathbb{R}^{d \times d} \text{ such that } \xi_{ij} = \xi_{ji} \neq 0. \end{aligned}$$

Here, and in the following, we use the convention of summation over the repeated indices. Note that the elasticity coefficients  $c_{ijkl} \in L^\infty(\Omega_\Sigma)$  allow to be anisotropic as well as discontinuous along  $\Sigma$ . The latter case implies the bond of dissimilar materials.

At the interface  $\Sigma$  we use decomposition of vectors into the normal and tangential components:

$$\begin{aligned} u_v &:= u_i v_i, \quad (u_\tau)_i := u_i - u_v v_i, \quad i = 1, \dots, d, \\ \sigma_v(u) &:= \sigma_{ij}(u) v_j v_i, \quad (\sigma_\tau(u))_i := \sigma_{ij}(u) v_j - \sigma_v(u) v_i. \end{aligned}$$

Further,  $[[\xi]] := \xi|_{\Sigma^+} - \xi|_{\Sigma^-}$  will denote the jump of  $\xi$  across  $\Sigma$ .

For the given volume force  $f=(f_1, \dots, f_d) \in L^2(\Omega)^d$  and the boundary traction  $g=(g_1, \dots, g_d) \in L^2(\Gamma_N)^d$ , we look for  $u \in H^1(\Omega_\Sigma)^d$  such that

$$-\sigma_{ij,j}(u) = f_i, \quad 1 = 1, \dots, d, \quad \text{in } \Omega_\Sigma, \tag{1a}$$

$$\sigma_{ij}(u) n_j = g_i, \quad 1 = 1, \dots, d, \quad \text{on } \Gamma_N, \tag{1b}$$

$$u = 0 \quad \text{on } \Gamma_D, \tag{1c}$$

$$\sigma_\tau(u)|_{\Sigma^+} = \sigma_\tau(u)|_{\Sigma^-} = 0, \quad \sigma_v(u)|_{\Sigma^+} = \sigma_v(u)|_{\Sigma^-}, \tag{1d}$$

$$[[u_v]] \geq 0, \quad \begin{cases} \sigma_v(u) \leq \gamma/\delta & \text{if } [[u_v]] = 0, \\ \sigma_v(u) = \gamma/\delta & \text{if } 0 < [[u_v]] \leq \delta, \\ \sigma_v(u) = 0 & \text{if } [[u_v]] > \delta \end{cases} \quad \text{on } \Sigma. \tag{1e}$$

While the standard linear elasticity relations (1a), (1b)–(1d) account respectively for the equilibrium equation and boundary conditions, relations (1e) describes plastic

deformation at the interface  $\Sigma$ . The parameters  $\delta > 0$  and  $\gamma > 0$  are given and the value of  $\gamma/\delta$  implies the elastic limit.

For comparison, within the frame of pure elasticity, the boundary conditions of contact [13] reads as

$$\llbracket u_v \rrbracket \geq 0, \quad \begin{cases} \sigma_v(u) \leq 0 & \text{if } \llbracket u_v \rrbracket = 0, \\ \sigma_v(u) = 0 & \text{if } \llbracket u_v \rrbracket > 0, \end{cases} \quad \text{on } \Sigma. \quad (1e')$$

The advantage of (1e) over (1e') lies in the fact that model (1) has a broad scope to prevent infinite stresses  $\sigma_v(u)$  at the interface, which would be inconsistent physically.

According to (1e), the interface  $\Sigma$  is open if  $\llbracket u_v \rrbracket > 0$ , otherwise closed. Moreover, the interface admits the tangential shear  $\llbracket u_\tau \rrbracket \neq 0$ . When both  $\llbracket u_v \rrbracket = 0$  and  $\llbracket u_\tau \rrbracket = 0$  at a subset  $\Gamma' \subseteq \Sigma$ , we refer to  $\Gamma'$  as an ideal bond. The complementary set  $\Gamma$  is referred to a crack. After finding a solution of (1), the (multi-) crack is determined by

$$\Gamma := \Sigma \setminus \Gamma', \quad \Gamma' := \{x \in \Sigma : \llbracket u(x) \rrbracket = 0\}.$$

This construction determines a defect (the crack  $\Gamma$ ) at the interface. Moreover, it allows us also to describe crack processing in time, which will be specified further in Section 5.

Next we get a weak formulation of problem (1). Observe that the function  $\llbracket u_v \rrbracket \mapsto \sigma_v(u)$  defined in (1e) obeys a discontinuity when  $\llbracket u_v \rrbracket = \delta$ . Using the Heaviside function

$$\mathcal{H}(\xi) := \begin{cases} 1 & \text{for } \xi \geq 0, \\ 0 & \text{for } \xi < 0, \end{cases}$$

relations (1e) can be expressed equivalently as the complementarity system

$$\begin{aligned} \frac{\gamma}{\delta} \mathcal{H}(\delta - \llbracket u_v \rrbracket) - \sigma_v(u) &\geq 0, \quad \llbracket u_v \rrbracket \geq 0, \\ \left(\frac{\gamma}{\delta} \mathcal{H}(\delta - \llbracket u_v \rrbracket) - \sigma_v(u)\right) \llbracket u_v \rrbracket &= 0. \end{aligned} \quad (2)$$

Now we introduce the Sobolev space due to the Dirichlet condition (1c)

$$H(\Omega_\Sigma) := \{v = (v_1, \dots, v_d) \in H^1(\Omega_\Sigma)^d : v = 0 \text{ on } \Gamma_D\},$$

and the convex cone of feasible displacements due to (1e)

$$K(\Sigma) := \{v \in H(\Omega_\Sigma) : \llbracket v_v \rrbracket \geq 0 \text{ on } \Sigma\}.$$

Multiplying (1a) with a test function  $v \in K(\Sigma)$ , integrating it by parts in  $\Omega_\Sigma$ , and accounting boundary relations (1b)–(1d) and (2), we arrive at the weak formulation of the boundary value problem (1): Find  $u \in K(\Sigma)$  such that

$$\begin{aligned} \int_{\Omega_\Sigma} (\sigma_{ij}(u) \varepsilon_{ij}(v - u) - f_i(v - u)_i) dx - \int_{\Gamma_N} g_i(v - u)_i dx \\ + \frac{\gamma}{\delta} \int_{\Sigma} \mathcal{H}(\delta - \llbracket u_v \rrbracket) \llbracket v_v - u_v \rrbracket dx \geq 0 \quad \text{for all } v \in K(\Sigma). \end{aligned} \quad (3)$$

Conversely, the  $H^2$ -smooth solution  $u$  of (3) fulfills relations (1) pointwise.

Note, that our modelling can be easily adapted to the obstacle (Signorini) problem, when  $\Sigma$  is a part of the outer boundary  $\partial\Omega$ . Under suitable geometric assumptions, one should just replace  $\Sigma^-$  with a rigid obstacle  $\psi$ , i.e.  $\llbracket u_v \rrbracket = u_n - \psi$  and  $\sigma_v(u) = -\sigma_n(u)$  at  $\Sigma = \Sigma^+$ , since  $v = -n$  in this case.

### 3. Primal-dual formulation of the crack problem

In this section we get variational principles for problem (3) which provide its solvability. In fact, we show that (3) implies a hemivariational inequality related to a nonsmooth minimization.

We start with obtaining a superpotential for the the Heaviside function  $\mathcal{H}$ . For this reason, let us define a continuous, nondifferentiable and concave function  $\xi \mapsto \beta(\xi) : \mathbb{R} \mapsto \mathbb{R}$  by

$$\beta(\xi) := \frac{\gamma}{\delta} \min(\delta, \xi) = \gamma \begin{cases} 1 & \text{for } \xi > \delta, \\ \xi/\delta & \text{for } \xi \leq \delta. \end{cases} \tag{4}$$

This function satisfies the concavity inequality

$$\beta(\eta) - \beta(\xi) \leq \frac{\gamma}{\delta} \mathcal{H}(\delta - \xi) (\eta - \xi) \quad \text{for } \xi, \eta \in \mathbb{R}. \tag{5}$$

From (5) it follows existence of the upper limit

$$\limsup_{t \rightarrow 0} \frac{\beta(\xi + t(\eta - \xi)) - \beta(\xi)}{t} \leq \frac{\gamma}{\delta} \mathcal{H}(\delta - \xi) (\eta - \xi),$$

which implies that  $(\gamma/\delta)\mathcal{H}(\delta - \xi)$  is a superdifferential; see the definition of superdifferentials in [20].

Using these relations we derive the following theorem.

**THEOREM 1** *The hemivariational inequality (3) yields the necessary optimality condition for the constrained minimization problem: Find  $u \in K(\Sigma)$  such that*

$$T(u) \leq T(v) \quad \text{for all } v \in K(\Sigma) \tag{6}$$

for the nonconvex and nondifferentiable objective (a superpotential)

$$\begin{aligned} T(v) &:= \Pi(v) + S(v), \quad S(v) := \int_{\Sigma} \beta(\llbracket v_v \rrbracket) dx, \\ \Pi(v) &:= \int_{\Omega_{\Sigma}} \left( \frac{1}{2} \sigma_{ij}(v) \varepsilon_{ij}(v) - f_i v_i \right) dx - \int_{\Gamma_N} g_i v_i dx. \end{aligned}$$

Moreover, problem (6), hence (3), obeys a solution.

*Proof* Firstly we derive (3) from (6). If (6) is satisfied, using (5) we infer that

$$\begin{aligned} \Pi(u) - \Pi(v) &\leq \int_{\Sigma} (\beta(\llbracket v_v \rrbracket) - \beta(\llbracket u_v \rrbracket)) dx \\ &\leq \frac{\gamma}{\delta} \int_{\Sigma} \mathcal{H}(\delta - \llbracket u_v \rrbracket) \llbracket v_v - u_v \rrbracket dx \quad \text{for all } v \in K(\Sigma). \end{aligned}$$

For arbitrary  $w \in K(\Sigma)$ , the substitution of  $v = tw + (1 - t)u \in K(\Sigma)$ ,  $t \in (0, 1)$ , gets

$$\frac{\Pi(u + t(w - u)) - \Pi(u)}{t} \geq -\frac{\gamma}{\delta} \int_{\Sigma} \mathcal{H}(\delta - \llbracket u_v \rrbracket) \llbracket w_v - u_v \rrbracket dx.$$

In view of the Gâteaux differentiability of  $u \mapsto \Pi(u)$ , we arrive at (3) by passing to the limit in the last inequality as  $t \rightarrow 0$ .

Second we justify the solvability of (6), hence (3). We observe that the functional  $T$  (of the total potential energy) is the sum of the potential energy  $\Pi$  and the surface (cohesive) energy  $S$  at the interface  $\Sigma$ . The cohesive energy is defined by the density function  $\beta$ , which is concave and nondifferentiable in our case. Nevertheless, due to the Lipschitz continuity of the nonnegative mapping  $\llbracket v_v \rrbracket \mapsto \beta(\llbracket v_v \rrbracket) : \mathbb{R}_+ \mapsto \mathbb{R}_+$  and the strict convexity of the quadratic functional  $v \mapsto \Pi$ , there exists a solution  $u$  to (6) (see the details in [15]). ■

Using Theorem 1 we can determine dual variables (the Lagrange multipliers). This goal needs to get a distributional sense for the boundary conditions at the interface  $\Sigma$ . Let  $H_{00}^{1/2}(\Sigma)$  denote the Lions–Magenes space of  $H^{1/2}$ -functions which admit the continuation by zero onto any closed surface, and  $H_{00}^{1/2}(\Sigma)^*$  be its dual space. Then the inclusion  $\llbracket u_v \rrbracket \in H_{00}^{1/2}(\Sigma)$  follows from the trace theorems [13] for cracked domains. The normal stress  $\sigma_v(u) \in H_{00}^{1/2}(\Sigma)^*$  is defined well by the following Green formula, for  $v \in H(\Omega_{\Sigma})$ ,

$$\langle \sigma_v(u), \llbracket v_v \rrbracket \rangle_{\Sigma} = \int_{\Omega_{\Sigma}} (f_i v_i - \sigma_{ij}(u) \varepsilon_{ij}(v)) dx + \int_{\Gamma_N} g_i v_i dx. \tag{7}$$

The brackets  $\langle \cdot, \cdot \rangle_{\Sigma}$  stands for the duality pairing between  $H_{00}^{1/2}(\Sigma)^*$  and  $H_{00}^{1/2}(\Sigma)$ . Henceforth, these arguments justify the inclusions

$$p := \frac{\gamma}{\delta} \mathcal{H}(\delta - \llbracket u_v \rrbracket) \in L^2(\Sigma), \quad \lambda := p - \sigma_v(u) \in H_{00}^{1/2}(\Sigma)^*. \tag{8}$$

With this notation, the complementarity conditions (2) hold as

$$\llbracket u_v \rrbracket \geq 0, \quad \langle \lambda, \llbracket v_v - u_v \rrbracket \rangle_{\Sigma} \geq 0 \quad \text{for all } v \in K(\Sigma). \tag{9}$$

Note that relations (7)–(9) are equivalent to the hemivariational inequality (3). To get a physical sense to the Lagrange multipliers  $\lambda$  and  $p$  defined in (8), we note that  $\lambda$  implies the contact force, while  $p$  describes the cohesion force between the surfaces  $\Sigma^{\pm}$ .

We remark that, if the solution  $u$  of (3) was unique, then the hemivariational inequality would yield the necessary and sufficient optimality condition for minimization problem (6). Generally, the sufficient condition is given in the following theorem.

**THEOREM 2** *The sufficient optimality condition for (6) yields the following minimax problem: Find  $(u, \lambda) \in H(\Omega_{\Sigma}) \times M_+$  such that*

$$\mathcal{L}(u, \mu) \leq \mathcal{L}(u, \lambda) \leq \mathcal{L}(v, \lambda) \quad \text{for all } (v, \mu) \in H(\Omega_{\Sigma}) \times M_+, \tag{10}$$

where the Lagrangian is given by

$$\mathcal{L}(v, \mu) := T(v) - \langle \mu, \llbracket v_v \rrbracket \rangle_\Sigma, \tag{11}$$

and the dual cone

$$M_+ = \{ \mu \in H_{00}^{1/2}(\Sigma)^* : \langle \mu, \xi \rangle_\Sigma \geq 0 \text{ for all } \xi \in H_{00}^{1/2}(\Sigma), \xi \geq 0 \}.$$

There exists a solution of (10), and its primal component  $u^* \in K(\Sigma)$  solves minimization problem (6).

*Proof* The solvability of (10) follows from the minimax theorems, e.g. adapting the proof of [4], and using the Lipschitz continuity of the function  $\beta(\xi)$  and  $\beta \geq 0$ .

Now we derive (6) from (10). From the left inequality in (10),

$$\lambda \in M_+, \quad \langle \mu - \lambda, \llbracket u_v \rrbracket \rangle_\Sigma \leq 0 \text{ for all } \mu \in M_+,$$

using the primal-dual complementarity arguments we infer (9). Henceforth,  $u \in K(\Sigma)$ , and the right inequality in (10) reads as

$$\mathcal{L}(u, \lambda) = T(u) \leq T(v) - \langle \lambda, \llbracket v_v \rrbracket \rangle_\Sigma = \mathcal{L}(v, \lambda) \text{ for all } v \in H(\Omega_\Sigma). \tag{12}$$

Substituting test functions  $v \in K(\Sigma)$  into (12) provides that  $u$  is a solution of the minimization problem (6). ■

Theorems 1 and 2 guarantee solvability of the hemivariational inequality (3). Indeed, solving the minimization problem (6) or the minimax problem (10) yields a solution to (3), too. The existing numerical methods realizes this approach based on the superpotential  $T$  [6,18]. However, a solution of the hemivariational inequality is not necessary a minimizer of  $T$  (see the example in [10]). We construct a numerical algorithm solving (3) directly.

#### 4. A primal-dual active set algorithm

In Section 4.1 we get a PDAS-algorithm for the numerical solution of the hemivariational inequality (3). In Section 4.2 we establish global and monotone properties of convergence of its iterates.

##### 4.1. Derivation of the algorithm

Let  $u^* \in K(\Sigma)$  be a solution of (3). Following the lines (7)–(9), we restate the hemivariational inequality in the primal-dual setting as

$$\int_{\Omega_\Sigma} (\sigma_{ij}(u^*) \varepsilon_{ij}(v) - f_i v_i) dx - \int_{\Gamma_N} g_i v_i dx + \langle p^* - \lambda^*, \llbracket v_v \rrbracket \rangle_\Sigma = 0$$

for all  $v \in H(\Omega_\Sigma)$ , (13)

$$p^* = \frac{\gamma}{\delta} \mathcal{H}(\delta - \llbracket u_v^* \rrbracket) \text{ at } \Sigma, \tag{14}$$

$$\llbracket u_v^* \rrbracket \geq 0, \quad \langle \lambda^*, \llbracket v_v - u_v^* \rrbracket \rangle_\Sigma \geq 0 \text{ for all } v \in K(\Sigma). \tag{15}$$



In order to endow the system (13)–(15) with an algorithmic form, in what follows we assume that the Lagrange multiplier  $\lambda^*$  admits a pointwise determination in the interior of  $\Sigma$ . This assumption has a sense within the interior  $H^{3/2}$ -smoothness of the solution  $u^*$  at  $\Sigma$  excepting the boundary  $\partial\Sigma$  (see justification of the smoothness in [16]). The boundary  $\partial\Sigma$  implies the front of  $\Sigma$  in  $\mathbb{R}^3$ , or its end points in  $\mathbb{R}^2$ . This assumption becomes trivial after discretization of the problem.

Below we derive a semi-Newton method for (13)–(15). While equation (13) is linear, it needs a proper approximation of nonlinear relations (14) and (15).

Due to the assumption, the complementarity conditions (15) can be represented in the pointwise sense, e.g., with the help of the ‘min’-based projection. For an arbitrarily fixed constant  $c > 0$  it reads as

$$\lambda^* + \min(0, c\llbracket u_v^* \rrbracket - \lambda^*) = 0 \quad \text{at } \Sigma. \tag{16}$$

The ‘min’-function yields the representation

$$\min(0, \xi) = \xi \chi(\xi), \quad \chi(\xi) := 1 - \mathcal{H}(\xi) \quad \text{for } \xi \in \mathbb{R}.$$

Using a slant derivative, the property of generalized differentiability

$$\|\min(0, y + h) - \min(0, y) - h \chi(y + h)\|_{L^p(\Sigma)} = o(\|h\|_{L^2(\Sigma)}) \tag{17}$$

holds for  $p > 2$  [7,11]. Therefore, the generalized Newton method applied to the nonlinear equation (16) follows the iteration step

$$\lambda^n + (c\llbracket u_v^n \rrbracket - \lambda^n) \chi(c\llbracket u_v^{n-1} \rrbracket - \lambda^{n-1}) = 0 \quad \text{at } \Sigma. \tag{18}$$

Estimate (17) implies that (18) is a superlinear approximation of (16), for the sufficiently smooth functions.

Since the other equation (14) is represented by the discontinuous function, we apply to it a linear approximation

$$p^n = \frac{\gamma}{\delta} \mathcal{H}(\delta - \llbracket u_v^{n-1} \rrbracket) \quad \text{at } \Sigma. \tag{19}$$

Thus, we arrive at the following iteration of problem (13)–(15). Given an initial  $(u^0, \lambda^0, p^0)$ , for  $n = 1, 2, \dots$  compute  $(u^n, \lambda^n, p^n)$  satisfying

$$\int_{\Omega_\Sigma} (\sigma_{ij}(u^n) \varepsilon_{ij}(v) - f_i v_i) dx - \int_{\Gamma_N} g_i v_i dx + \langle p^n - \lambda^n, \llbracket v_v \rrbracket \rangle_\Sigma = 0$$

for all  $v \in H(\Omega_\Sigma)$ , and the conditions (18) and (19) at  $\Sigma$ . (20)

Now we apply arguments of active sets to problem (13)–(15) and its iteration (20). We partition  $\Sigma$  into active sets  $A$  and complementary inactive sets either with respect to the contact conditions (16) by

$$A_c^* := \{x \in \Sigma : (c\llbracket u_v^* \rrbracket - \lambda^*)(x) < 0\}, \tag{21}$$

or with respect to the cohesion force (14) by

$$A_p^* := \{x \in \Sigma : \llbracket u_v^* \rrbracket(x) \leq \delta\}. \tag{22}$$

The former partition (21) implies strong contact between the surfaces  $\Sigma^\pm$  at the active set  $A_c^*$ , i.e.  $\llbracket u_v^* \rrbracket = 0$  and  $\lambda^* > 0$ . The latter partition (22) describes the cohesion at the part  $A_p^*$  of the interface  $\Sigma$ , and no cohesion at  $\Sigma \setminus A_p^*$ .

With the definition of the active sets in (21) and (22), the primal-dual system (13)–(15) turns to the equivalent relations:

$$\int_{\Omega_\Sigma} (\sigma_{ij}(u^*)\varepsilon_{ij}(v) - f_i v_i) dx - \int_{\Gamma_N} g_i v_i dx + \langle p^* - \lambda^*, \llbracket v_v \rrbracket \rangle_\Sigma = 0$$

for all  $v \in H(\Omega_\Sigma)$ ,

(23a)

$$p^* = \gamma/\delta \quad \text{on } A_p^*, \quad p^* = 0 \quad \text{on } \Sigma \setminus A_p^*,$$
(23b)

$$\llbracket u_v^* \rrbracket = 0 \quad \text{on } A_c^*, \quad \lambda^* = 0 \quad \text{on } \Sigma \setminus A_c^*.$$
(23c)

Similarly, iteration (20) forces the PDAS-algorithm:

*Algorithm 1*

- (0) Choose initializations  $A_c^{-1}$  and  $A_p^{-1}$  at  $\Sigma$ ; set  $n = 0$ .
- (1) Solve for  $(u^n, \lambda^n, p^n)$  the linear system:

$$\int_{\Omega_\Sigma} (\sigma_{ij}(u^n)\varepsilon_{ij}(v) - f_i v_i) dx - \int_{\Gamma_N} g_i v_i dx + \langle p^n - \lambda^n, \llbracket v_v \rrbracket \rangle_\Sigma = 0$$

for all  $v \in H(\Omega_\Sigma)$ ,

(24a)

$$p^n = \gamma/\delta \quad \text{on } A_p^{n-1}, \quad p^n = 0 \quad \text{on } \Sigma \setminus A_p^{n-1},$$
(24b)

$$\llbracket u_v^n \rrbracket = 0 \quad \text{on } A_c^{n-1}, \quad \lambda^n = 0 \quad \text{on } \Sigma \setminus A_c^{n-1}.$$
(24c)

- (2) Compute the active sets at  $(u^n, \lambda^n)$ :

$$A_c^n = \{x \in \Sigma : (c \llbracket u_v^n \rrbracket - \lambda^n)(x) < 0\},$$
(25a)

$$A_p^n = \{x \in \Sigma : \llbracket u_v^n \rrbracket(x) \leq \delta\}.$$
(25b)

- (3) If  $A_c^n = A_c^{n-1}$  and  $A_p^n = A_p^{n-1}$  then STOP; else set  $n = n + 1$  and go to Step 1.

Given  $A_c^{n-1}$  and  $p^n$  in (24b) from the  $n - 1$  iteration, for every  $n \geq 0$  problem (24) is equivalent to a minimization of the quadratic functional

$$\int_{\Omega_\Sigma} \left( \frac{1}{2} \sigma_{ij}(v)\varepsilon_{ij}(v) - f_i v_i \right) dx - \int_{\Gamma_N} g_i v_i dx + \langle p^n, \llbracket v_v \rrbracket \rangle_{\Sigma \setminus A_c^{n-1}}$$

over admissible functions  $v \in H(\Omega_\Sigma)$  such that  $\llbracket v_v \rrbracket = 0$  at  $A_c^{n-1}$ . This convex minimization problem obeys the unique minimizer  $u^n$ . It determines  $\lambda^n = p^n - \sigma_v(u^n)$  at  $\Sigma$ . Thus, (24) is well posed.

The stopping rule is motivated by the following.

PROPOSITION 1 *If  $A_c^n = A_c^{n-1}$  and  $A_p^n = A_p^{n-1}$  in Algorithm 1, then  $(u^n, \lambda^n, p^n) = (u^*, \lambda^*, p^*)$ .*

*Proof* If  $A_c^n = A_c^{n-1}$ , then from (24c) and (25a) it follows that  $\llbracket u_v^n \rrbracket \geq 0$  and  $\lambda^n \geq 0$  fulfill pointwise the complementarity condition (15). If  $A_p^n = A_p^{n-1}$ , then  $p^n = \gamma/\delta \mathcal{H}(\delta - \llbracket u_v^n \rrbracket)$ , that implies (14). Thus, such iterates  $(u^n, \lambda^n, p^n)$  satisfy the desired system (13)–(15), equivalently, (21)–(23). ■

While the approximation (18) is more regular than (19), a faster convergence of the contact set  $A_c^n$  over the cohesion set  $A_p^n$  is foreseen. Nevertheless, the accuracy of  $\llbracket u_v^n \rrbracket$  speeds up the convergence of  $A_p^n$  by means of (25b). Indeed, from numerical computations we report the following. In our tests, Algorithm 1 always stopped successfully by coincidence of two consequent iterates, thus finding the exact solution of a discretized problem (13–15). The number of iterations required to attain the stopping rule is moderate.

#### 4.2. The convergence analysis

We investigate Algorithm 1 with respect to properties of global convergence of its iterates. It needs the following assumption.

*Assumption 1* During the iteration  $n = 1, 2, \dots$  of Algorithm 1,

$$\text{if } \sigma_v(u^n - u^{n-1}) \leq 0, \text{ then } \llbracket u_v^n - u_v^{n-1} \rrbracket \geq 0 \text{ at } \Sigma \setminus A_c^{n-1}. \tag{26}$$

Property (26) is related to a maximum principle for the mixed problem (24a). Thus, in Appendix we prove (26) for an asymptotic model of (24) within a three-dimensional elasticity. The proof is based on a Papkovitch–Neuber representation of the solution *via* harmonic potentials, which obey the maximum principle. For this topic we refer to [9]. After discretization of the problem, (26) is related to a M-property of the stiffness matrix (see the respective investigation in [8]).

Based on the assumption (26) we start with an auxiliary lemma, which establishes monotone properties of the sequence of iterates in Algorithm 1. The lemma uses a conception of feasible iterates. We refer to an iterate  $u^n$  as feasible, if  $\llbracket u_v^n \rrbracket \geq 0$  at  $\Sigma$ .

LEMMA 1 *Let Assumption 1 hold during the iteration  $n = 1, 2, \dots$*

(i) *If there exists  $n_1 \geq 1$  such that*

$$p^{n_1-1} \geq p^{n_1} \text{ at } \Sigma \setminus A_c^{n_1-1}, \tag{27}$$

*then for all  $n \geq n_1$  the iterates obey the following properties at  $\Sigma$ :*

$$\llbracket u_v^{n-1} \rrbracket \leq \llbracket u_v^n \rrbracket, \tag{28a}$$

$$p^n \geq p^{n+1}, \tag{28b}$$

$$A_p^n \supseteq A_p^{n+1}. \tag{28c}$$

(ii) If there exists  $n_2 \geq n_1$  such that  $u^{n_2}$  is feasible, then for all  $n \geq n_2$  the iterates  $u^n$  are feasible, and

$$A_c^{n-1} \supseteq A_c^n. \tag{29}$$

*Proof* We start to prove the assertion (i). During the iteration (24c), either  $\llbracket u_v^{n-1} \rrbracket = 0$ , or  $\lambda^{n-1} = 0$ . Therefore, from (25a) we observe that  $\llbracket u_v^{n-1} \rrbracket \leq 0$  at  $A_c^{n-1}$ . Since  $\llbracket u_v^n \rrbracket = 0$  at  $A_c^{n-1}$ , we conclude that

$$\llbracket u_v^n - u_v^{n-1} \rrbracket \geq 0 \text{ at } A_c^{n-1} \text{ for all } n \geq 1. \tag{30}$$

Next we consider  $\Sigma \setminus A_c^{n-1}$ . It is useful to rewrite (26) in Assumption 1 using the representation  $\sigma_v(u) = p - \lambda$  as

$$p^n - p^{n-1} - (\lambda^n - \lambda^{n-1}) \leq 0 \Rightarrow \llbracket u_v^n - u_v^{n-1} \rrbracket \geq 0 \text{ at } \Sigma \setminus A_c^{n-1}. \tag{31}$$

From (24c) and (25a) we find that  $\lambda^{n-1} \leq 0 = \lambda^n$  at  $\Sigma \setminus A_c^{n-1}$ , and

$$\lambda^n - \lambda^{n-1} \geq 0 \text{ at } \Sigma \setminus A_c^{n-1} \text{ for all } n \geq 1. \tag{32}$$

Using (32), if  $p^n - p^{n-1} \geq 0$  holds for a fixed  $n = n_1$  in (27), then (31) ensures that  $\llbracket u_v^n - u_v^{n-1} \rrbracket \geq 0$  at  $\Sigma \setminus A_c^{n-1}$ . This together with (30) results in the inequality (28a). The definition of iterates of  $p$  in (19) follows immediately properties (28b) and (28c) provided by (28a). Finally, we employ the induction arguments for  $n > n_1$ .

Now, we justify the assertion (ii). Let  $u^{n-1}$  be feasible. Then (28a) implies that  $u^n$  is feasible. For  $\llbracket u_v^n \rrbracket \geq 0$ , (25a) ensures the inclusion asserted in (29). ■

Based on Lemma 1, for a specific initialization below we guarantee the monotony of the sequence  $\{\llbracket u_v^n \rrbracket, p^n, A_p^n, A_c^n\}$  for  $n = 1, 2, \dots$

**PROPOSITION 2** Under Assumption 1, for the initialization  $A_c^{-1} = \emptyset$  and  $A_p^{-1} = \Sigma$ , the iterates of Algorithm 1 obey the following monotone properties:

$$0 \leq \llbracket u_v^1 \rrbracket \leq \dots \leq \llbracket u_v^{n-1} \rrbracket \leq \llbracket u_v^n \rrbracket, \tag{33a}$$

$$1 \equiv p^0 \geq p^1 \geq \dots \geq p^{n-1} \geq p^n, \tag{33b}$$

$$\Sigma = A_p^{-1} \supseteq A_p^0 \supseteq \dots \supseteq A_p^{n-1} \supseteq A_p^n, \tag{33c}$$

$$\Sigma \supseteq A_c^0 \supseteq \dots \supseteq A_c^{n-1} \supseteq A_c^n. \tag{33d}$$

*Proof* Indeed, for the initialization  $A_p^{-1} = \Sigma$  we have  $p^0 = \gamma/\delta$  at  $\Sigma$ . Therefore, the estimate  $0 \leq p^1 \leq \gamma/\delta$  ensures (27) and the assertion (i) in Lemma 1 with  $n_1 = 1$ .

For the initialization  $A_c^{-1} = \emptyset$  we have  $\lambda^0 = 0$  at  $\Sigma$ . The respective partition of  $\Sigma$  implies that  $\llbracket u_v^0 \rrbracket < 0$  at  $A_c^0$ , and  $\llbracket u_v^0 \rrbracket \geq 0$  at  $\Sigma \setminus A_c^0$ . Therefore,  $\llbracket u_v^1 \rrbracket \geq \llbracket u_v^0 \rrbracket \geq 0$  at  $\Sigma \setminus A_c^0$  due to (28a). Moreover,  $\llbracket u_v^1 \rrbracket = 0$  at  $A_c^0$  in view of (24c). Thus, the iterate  $u^1$  is feasible, and the assertion (ii) in Lemma 1 holds true for  $n_2 = 1$ . ■

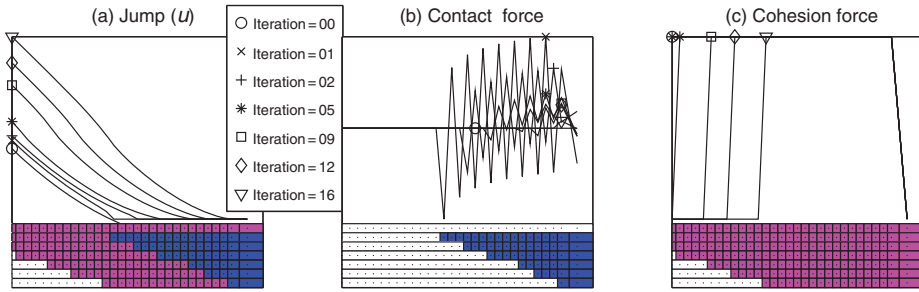


Figure 1. Example history of the iterates of Algorithm 1.

Note that, avoiding the specific initialization given in Proposition 2, the monotone properties (33) of the sequence  $\{\llbracket u_v^n \rrbracket, p^n, A_p^n, A_c^n\}$  can be restated for  $n \geq n_2$ , if  $n_1$  and  $n_2$  in Lemma 1 exist. However, no monotony is guaranteed until Algorithm 1 attains such a feasible iterate  $u^{n_2}$  that  $p^{n_2} \leq p^{n_2-1}$  at  $\Sigma \setminus A_c^{n_2-1}$ .

We stress that the sequence of iterates  $\{\lambda^n\}$  need not be monotone. As a consequence, no convergence  $(u^n, \lambda^n, p^n) \rightarrow (u^*, \lambda^*, p^*)$  as  $n \rightarrow \infty$  can be assured in the continuous setting of the problem. Nevertheless, the monotony of active sets in a finite-dimensional space guarantees that the stopping rule in Algorithm 1 is attained after a finite number of iterations. Thus, upon a proper discretization, Propositions 1 and 2 ensure that there exists a finite  $n^* \in \mathbb{N}$  such that  $(u^{n^*}, \lambda^{n^*}, p^{n^*}) = (u^*, \lambda^*, p^*)$ .

From our numerical tests we report on the following features.

The typical history of iterates of the PDAS-algorithm is depicted in Figure 1 at the selected iterates  $n$ . Below bars show history during the iteration of the active sets  $A_c^n$  in subplot (b),  $A_p^n$  in subplot (c), and both as the stack of bars in subplot (a). From this plot we observe globally: the monotone increases for the constrained component of the jump  $\llbracket u_v^n \rrbracket$  in subplot (a), the monotone decreases for the cohesion force  $p^n$  in subplot (c), the monotone decreases for the active sets  $A_c^n$  and  $A_p^n$ , but there is no monotony for the Lagrange multiplier (contact force)  $\lambda^n$  in subplot (b). The numerical features justify our theoretical assertion in (33). For the numerical tests we took the constant  $c = 10^{-8}$ .

For adaptive remeshing we use a nested technique. It implies an extension of the active sets from a coarse grid to initialize the algorithm on a fine grid. To get the adaptive meshes we use the error estimator  $\eta$  over a triangular mesh  $\{T\}$

$$\eta_{\{T\}}^2 = \sum_{\{T\}} \eta_T^2, \quad \eta_T^2 = \eta_{T^o}^2 + \eta_{\partial T}^2 + \eta_{\Sigma}^2, \tag{34}$$

which is based on the strong formulation (1), with the terms:

$$\eta_{T^o}^2 = \text{diam}(T)^2 \sum_{i=1}^d \|\sigma_{ij,j}(u^*) - f_i\|_{L^2(T)}^2,$$

$$\eta_{\partial T}^2 = \text{diam}(\partial T) \sum_{i=1}^d \left( \frac{1}{2} \|\llbracket \sigma_{ij}(u^*) \rrbracket n_j\|_{L^2(\partial T \cap \Omega)}^2 + \|\sigma_{ij}(u^*) n_j - g_i\|_{L^2(\partial T \cap \Gamma_N)}^2 \right),$$

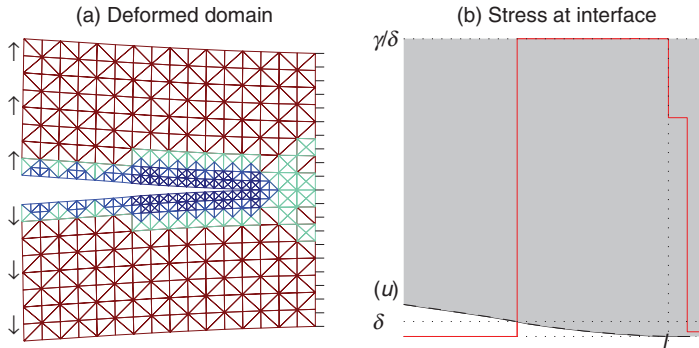


Figure 2. Solution of the crack problem at  $q=0.05621$ .

$$\eta_{\Sigma}^2 = \text{diam}(\partial T) \left( \sum_{i=1}^d \|\sigma_{\tau}(u^*)\|_{L^2(\partial T \cap \Sigma^{\pm})}^2 + \|\llbracket \sigma_{\nu}(u^*) \rrbracket\|_{L^2(\partial T \cap \Sigma)}^2 + \|p^* - \sigma_{\nu}(u^*)\|_{L^2(\partial T \cap \Sigma \setminus A_p^*)}^2 + \|\sigma_{\nu}(u^*) + \lambda^*\|_{L^2(\partial T \cap \Sigma \setminus A_p^*)}^2 \right).$$

The notation  $\llbracket \sigma_{ij}(u^*) \rrbracket n_j$  implies the jump across the boundary  $\partial T$  of joint triangles, and  $n$  stands here for the unit normal at  $\partial T$ . The adaptive remeshing technique reduces costly fine-grid iterations. An example of the adaptive mesh is illustrated in Figure 2(a).

Using the PDAS-algorithm incorporated into the adaptive finite-element method for the numerical calculation, we further investigate a physical matter of the hemivariational inequality.

### 5. A numerical example of the quasibrittle fracture

In this section we describe a quasibrittle fracture. For the reason of physical consistency,  $\Sigma$  assumes a prescribed interface between two similar or dissimilar materials. Further, we consider problem (1) under a time-dependent loading. Since the quasibrittle model admits closing of the crack faces, the loading needs not be monotone in time. As the consequence, we can describe similarly the processes of bonding (closing the crack) as well as debonding (opening the crack) along the fixed interface. By this formulation, a cracking across the interface is not allowed.

In the example below we rely on the isotropic material characterized by the Lamé parameters  $\mu = \frac{E}{2(1+\kappa)}$  and  $\lambda = \frac{2\kappa\mu}{1-2\kappa}$ . The Young modulus  $E=73000$  (mPa) and the Poisson ratio  $\kappa=0.34$  are taken. For other material parameters we set  $\gamma=10$  (mPa m) and  $\delta=0.01$  (m).

Using a plane deformation assumptions, we consider the cross-section  $\Omega=(0, 1)^2$  of the solid body. We assume that no volume forces are applied. Let the right edge be clamped as  $x_1=1$ . For a loading parameter  $q \geq 0$  we consider the traction given at

the left edge (as  $x_1 = 0$ ) by

$$g_1(x_2) \equiv 0, \quad g_2(x_2) = \pm q\mu \quad \text{for } x_2 > \pm 0.5.$$

Due to the reflection symmetry of the specific data of the problem, heuristic arguments suggest interface  $\Sigma$  as the median line  $x_2 = 0.5$  for  $x_1 \in (0, 1)$ . This suggestion is reasonable physically. Indeed, after solving the equilibrium problem we find that the stress intensity factor  $K_{II} = 0$  at  $\Sigma$ , which prevents the pre-assigned interface from a kink.

In such  $\Omega_\Sigma$  with the plane interface,  $\tau = (1, 0)$  in (1d),  $\nu = (0, 1)$  in (1e) and (1a) turns into the standard Lamé equations. After a linear finite-element discretization, the respective problem (1) is solved with the help of Algorithm 1. The inner-loop iteration for the linear problem (24) was stopped with  $\text{tol} = 10^{-10}$ . The reference solution at  $q = 0.05621$  is depicted in Figure 2.

The left subplot (a) presents the domain  $\Omega_\Sigma$  deformed with the displacement  $u^*$ , which is scaled by the factor 5 for visual clarity. The adaptive mesh is produced using the error estimator  $\eta_{\{T\}}$  from (34). For the visualization,  $\text{DOF} = 924$  is depicted. From our numerical tests we report on two principal zones subject to the adaptive refinement: a fine-mesh strip surrounding the open part of the interface  $\Sigma$ , and a local zone around the points separating active and inactive sets at  $\Sigma$ .

In the right plot (b), the normal stress  $\sigma_{22}(u^*)$  together with the jump of the normal displacement  $\llbracket u_2^* \rrbracket$  (which is scaled by the factor 5000) are depicted along the interface. In this plot we can observe the zone of plastic deformations where  $\sigma_{22}(u^*) = \gamma/\delta$  attains the elastic limit. It prevents the solution from infinite stresses at the interface.

For comparison, we computed the brittle model of Griffith ignoring the cohesion force. For this configuration, when putting  $p^* = 0$  in (23), we found that the interface was completely open for any  $q > 0$ . Thus, in the brittle model  $\Sigma$  described a fixed crack in  $\Omega$ .

In contrast, the quasibrittle model allows closing of the interface. Moreover, for every fixed  $q$  the active-set approach determines exactly the points  $x_1$  which separate the closed part of the interface (where  $\llbracket u_2^* \rrbracket(x_1) = 0$ ) from the open one (where  $\llbracket u_2^* \rrbracket(x_1) > 0$ ). Since  $\llbracket u_1^* \rrbracket \equiv 0$  in the symmetric example, we identify an interface crack as the following set:

$$\Gamma(q) = [0, 1] \setminus \Gamma'(q), \quad \Gamma'(q) := \{x_1 \in [0, 1] : \llbracket u_2^* \rrbracket(x_1) = 0\}. \tag{35}$$

For example, as  $q = 0.05621$ , from Figure 2 we find the one point  $l = 0.875$  such that  $\llbracket u_2^* \rrbracket(x_1) > 0$  for  $x_1 \in [0, l)$ , and  $\llbracket u_2^* \rrbracket(x_1) = 0$  for  $x_1 \in [l, 1]$ . This point determines, uniquely, the interface crack  $\Gamma(q)$  of the length  $l$  from (35).

In the following, we investigate our model with respect to the values  $q \in \mathbb{R}_+$  of the applied load  $q\mu$ . Solving the static problem at selected points within the interval  $q \in [0, 0.08]$  gets us the approximation of the function of the crack length  $l(q) \in [0, 1]$ , which is depicted in Figure 3. From this plot we observe that a macro-crack appears at the left end-point  $x_1 = 0$  of the interface, under a finite (nonzero) load  $q_0\mu$  with  $q_0 \approx 0.008$ . When increasing the load  $q\mu > q_0\mu$ , the interface crack becomes larger

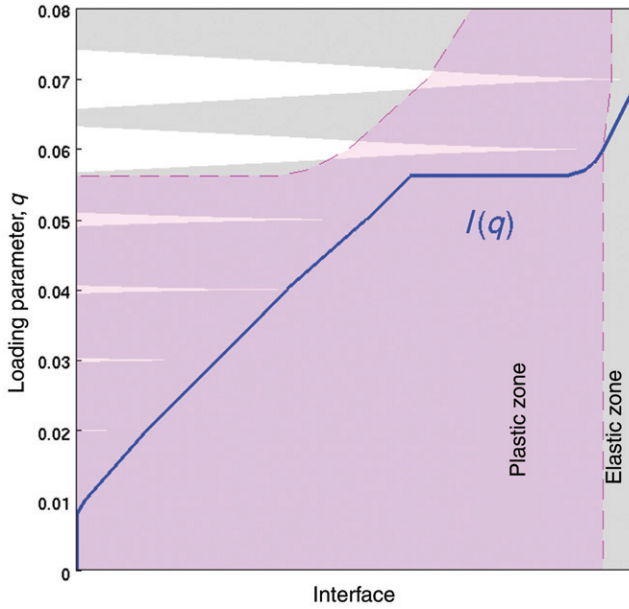


Figure 3. The length  $l(q) \in [0, 1]$  of the quasibrittle crack.

and approaches the right end-point  $x_1 = 1$ , which is posed at the clamped boundary. In this plot we also mark the location of the plastic zone at the interface in contrast to the elastic zone.

By the above considerations, from (35) we get the interface crack  $\Gamma(l(q))$  with respect to the length parameter  $l(q)$ . We emphasize that the stress intensity factors  $K_I$  and  $K_{II}$  at the respective crack tip  $x_1 = l(q)$  are zero. While the latter  $K_{II} = 0$  in view of  $[[u_1^*]] = 0$  at the crack, the former  $K_I = 0$  because of the closed faces at the crack tip (it can be viewed in Figure 2(b)). Indeed, the absence of singularity of  $[[u_2^*]]$  is guaranteed by the fulfillment of cohesion conditions at  $\Sigma$  [16]. Therefore,  $\Gamma(l(q))$  satisfy the fracture criterion:

$$\text{For every } q \geq 0, \text{ find a crack } \Gamma \subseteq \Sigma \text{ such that } K_I = 0.$$

This local criterion is intrinsic for the quasibrittle fracture.

For the time  $t \geq 0$ , we assume that  $t \mapsto q(t)$  describing a loading process in time. By this we make no assumptions on the mapping  $q(t)$ , thus allowing it to be a set-valued. Since the above results hold true regardless of the loading history  $q(t)$ , we can consider a monotone loading  $q(t) \nearrow$ , as well as a monotone unloading  $q(t) \searrow$ , and mixed loading processes. Note that, when unloading, no residual stress occurs due to the elasticity constitutive law holding in  $\Omega_\Sigma$ .

All these quasibrittle features are of importance in a fracture situation where the standard Griffiths brittle model is inapplicable.



## 6. Conclusion

Our PDAS approach provides suitable analytical as well as numerical tools for solution of hemivariational inequalities, in particular, in the presented context of crack problems.

## Acknowledgements

The research results were obtained with the support of the Austrian Science Fund (FWF) (project P21411-N13), the Russian Foundation for Basic Research (project 10-01-00054) and the Siberian Branch of the Russian Academy of Sciences (project N 90).

## References

- [1] C.C. Baniotopoulos, J. Haslinger, and Z. Moravkova, *Mathematical modelling of delamination and nonmonotone friction problems by hemivariational inequalities*, Appl. Math. 50 (2005), pp. 1–25.
- [2] R.S. Burachik and A.N. Iusem, *Set-Valued Mappings and Enlargements of Monotone Operators*, Springer, New York, 2008.
- [3] M. Charlotte, G. Francfort, J.-J. Marigo, and L. Truskinovsky, *Revisiting brittle fracture as an energy minimization problem: Comparison of Griffith and Barenblatt surface energy models*, in Proceedings of the Symposium on Continuous Damage and Fracture, Cachan 2000, A. Benallal, ed., The Data Science Library, Elsevier, Paris, 2000, pp. 7–12.
- [4] I. Ekeland and R. Témam, *Convex Analysis and Variational Problems*, SIAM, Philadelphia, PA, 1999.
- [5] D. Goeleven, D. Motreanu, Y. Dumont, and M. Rochdi, *Variational and Hemivariational Inequalities: Theory, Methods and Applications*, Kluwer, Boston, 2003.
- [6] J. Haslinger, M. Miettinen, and P.D. Panagiotopoulos, *Finite Element Method for Hemivariational Inequalities: Theory, Methods and Applications*, Kluwer, Dordrecht, 1999.
- [7] M. Hintermüller, K. Ito, and K. Kunisch, *The primal-dual active set strategy as a semismooth Newton method*, SIAM J. Optim. 13 (2003), pp. 865–888.
- [8] M. Hintermüller, V.A. Kovtunenکو, and K. Kunisch, *The primal-dual active set method for a crack problem with non-penetration*, IMA J. Appl. Math. 69 (2004), pp. 1–26.
- [9] M. Hintermüller, V.A. Kovtunenکو, and K. Kunisch, *A Papkovich–Neuber-based numerical approach to cracks with contact in 3D*, IMA J. Appl. Math. 74 (2009), pp. 325–343.
- [10] M. Hintermüller, V.A. Kovtunenکو, and K. Kunisch, *Obstacle problems with cohesion: A hemi-variational inequality approach and its efficient numerical solution*, MATHEON Rep., Vol. 687, DFG-Forschungszentrum, TU-Berlin, 2010.
- [11] K. Ito and K. Kunisch, *Semi-smooth Newton methods for the variational inequalities of the first kind*, ESAIM Math. Model. Numer. Anal. 37 (2003), pp. 41–62.
- [12] H. Itou, V.A. Kovtunenکو, and A. Tani, *The interface crack with Coulomb friction between two bonded dissimilar elastic media*, Research Report KSTS/RR-10, Department of Mathematics, Keio University, Yokohama, 2010.
- [13] A.M. Khludnev and V.A. Kovtunenکو, *Analysis of Cracks in Solids*, WIT-Press, Southampton, Boston, 2000.
- [14] D. Klatte and B. Kummer, *Nonsmooth Equations in Optimization*, Kluwer, Dordrecht, 2002.

[15] V.A. Kovtunenکو, *Nonconvex problem for crack with nonpenetration*, Z. Angew. Math. Mech. 85 (2005), pp. 242–251.  
 [16] V.A. Kovtunenکو and I.V. Sukhorukov, *Optimization formulation of the evolutionary problem of crack propagation under quasibrittle fracture*, Appl. Mech. Tech. Phys. 47 (2006), pp. 704–713.  
 [17] A.S. Kravchuk, *Variational and Quasivariational Inequalities in Mechanics*, MGAPI, Moscow, 1997 [in Russian].  
 [18] M.M. Mäkelä, M. Miettinen, L. Lukšan, and J. Vlček, *Comparing nonsmooth nonconvex bundle methods in solving hemivariational inequalities*, J. Global Optim. 14 (1999), pp. 117–135.  
 [19] J.-J. Marigo and L. Truskinovsky, *Initiation and propagation of fracture in the models of Griffith and Barenblatt*, Contin. Mech. Thermodyn. 16 (2004), pp. 391–409.  
 [20] B.S. Mordukhovich, *Subdifferential and superdifferential optimality conditions in non smooth minimization*, Research Rep., Vol. 4, Department of Mathematics, Wayne State University, 2003.  
 [21] B.S. Mordukhovich, *Variational Analysis and Generalized Differentiation*, Springer-Verlag, Berlin, 2006.  
 [22] N.F. Morozov and Yu.V. Petrov, *Dynamics of Fracture*, Springer, Berlin, 2000.  
 [23] Z. Naniewicz and P.D. Panagiotopoulos, *Mathematical Theory of Hemivariational Inequalities and Applications*, Dekker, New York, 1995.  
 [24] R.T. Rockafellar and R.J.-B. Wets, *Variational Analysis*, Springer, Berlin, 1998.  
 [25] M.V. Solodov and B.F. Svaiter, *A truly globally convergent Newton-type method for the monotone nonlinear complementarity problem*, SIAM J. Optim. 10 (2000), pp. 605–625.

**Appendix**

We prove (26) in Assumption 1 for an asymptotic model stated in the infinite space  $\mathbb{R}^3$ . For this aim, we consider the three-dimensional isotropic equations

$$\sigma_{ij}(u) = 2\mu\varepsilon_{ij}(u) + \lambda\delta_{ij}\text{div}(u) \quad \text{for } i, j = 1, 2, 3,$$

given by the Lamé parameters  $\lambda > 0, \mu > 0$ , and the interface  $\Sigma$  expressed as the infinite plane  $\{x_3 = 0\}$ , that is

$$\Sigma = \{x = (\bar{x}, 0) \text{ for } \bar{x} = (x_1, x_2) \in \mathbb{R}^2\}.$$

The asymptotic model of problem (23) reads as

$$\begin{aligned} -\mu\Delta u^* - (\mu + \lambda)\nabla(\text{div } u^*) &= f && \text{in } \mathbb{R}^3 \setminus \Sigma, \\ \sigma_{13}(u^*) = \sigma_{23}(u^*) &= 0 && \text{on } \Sigma^\pm, \\ u^*(x) &= o(1) && \text{as } |x| \rightarrow \infty, \\ \llbracket u_3^* \rrbracket(\bar{x}, 0) &= 0 && \text{for } \bar{x} \in A_c^*, \\ \sigma_{33}(u^*)(\bar{x}, 0) &= p^*(\bar{x}) && \text{for } \bar{x} \in \mathbb{R}^2 \setminus A_c^*, \\ A_c^* &= \{\bar{x} \in \mathbb{R}^2 : c\llbracket u_3^* \rrbracket(\bar{x}, 0) - \lambda^*(\bar{x}) < 0\}, \end{aligned} \tag{36}$$

where the Lagrange multipliers are determined for  $\bar{x} \in \mathbb{R}^2$  as

$$p^*(\bar{x}) = \frac{\gamma}{\delta} \mathcal{H}(\delta - \llbracket u_3^* \rrbracket(\bar{x}, 0)), \quad \lambda^*(\bar{x}) = p^*(\bar{x}) - \sigma_{33}(u^*)(\bar{x}, 0).$$

Applying Algorithm 1 to (36) and given  $p^0, A_c^{-1}$ , for  $n=0, 1, \dots$ , we have to solve the mixed boundary-value problem

$$\begin{aligned}
 -\mu\Delta u^n - (\mu + \lambda)\nabla(\operatorname{div} u^n) &= f && \text{in } \mathbb{R}^3 \setminus \Sigma, \\
 \sigma_{13}(u^n) = \sigma_{23}(u^n) &= 0 && \text{on } \Sigma^\pm, \\
 u^n(x) &= o(1) && \text{as } |x| \rightarrow \infty, \\
 \llbracket u_3^n \rrbracket(\bar{x}, 0) &= 0 && \text{for } \bar{x} \in A_c^{n-1}, \\
 \sigma_{33}(u^n)(\bar{x}, 0) &= p^n(\bar{x}) && \text{for } \bar{x} \in \mathbb{R}^2 \setminus A_c^{n-1},
 \end{aligned} \tag{37}$$

during the iteration of the true active in  $\Sigma$  as

$$A_c^n = \{\bar{x} \in \mathbb{R}^2 : c\llbracket u_3^n \rrbracket(\bar{x}, 0) - \lambda^n(\bar{x}) < 0\}. \tag{38}$$

The respective Lagrange multipliers are found for  $\bar{x} \in \mathbb{R}^2$  by formula,

$$p^n(\bar{x}) = \frac{\gamma}{\delta} \mathcal{H}(\delta - \llbracket u_3^{n-1} \rrbracket(\bar{x}, 0)), \quad \lambda^n(\bar{x}) = p^n(\bar{x}) - \sigma_{33}(u^n)(\bar{x}, 0).$$

In the following, for  $n \geq 1$  we prove that

$$\text{if } \sigma_{33}(u^n - u^{n-1}) \leq 0, \text{ then } \llbracket u_3^n - u_3^{n-1} \rrbracket \geq 0 \text{ at } \mathbb{R}^2 \setminus A_c^{n-1}. \tag{39}$$

Let us denote  $\bar{u} := u^n - u^{n-1}$ . The difference of iterates in (37) for  $n$  and  $n - 1$  implies that

$$\begin{aligned}
 -\mu\Delta \bar{u} - (\mu + \lambda)\nabla(\operatorname{div} \bar{u}) &= 0 && \text{in } \mathbb{R}^3 \setminus \Sigma, \\
 \sigma_{13}(\bar{u}) = \sigma_{23}(\bar{u}) &= 0 && \text{on } \Sigma^\pm, \\
 \bar{u}(x) &= o(1) && \text{as } |x| \rightarrow \infty, \\
 \llbracket \bar{u}_3 \rrbracket(\bar{x}, 0) &= -\llbracket u_3^{n-1} \rrbracket(\bar{x}, 0) && \text{for } \bar{x} \in A_c^{n-1}, \\
 \sigma_{33}(\bar{u})(\bar{x}, 0) &= (p^n - p^{n-1} + \lambda^{n-1})(\bar{x}) && \text{for } \bar{x} \in \mathbb{R}^2 \setminus A_c^{n-1}.
 \end{aligned} \tag{40}$$

In  $\mathbb{R}_+^3$ , where  $x_3 > 0$ , we define the following functions

$$\begin{aligned}
 v_\alpha(x) &:= \bar{u}_\alpha(\bar{x}, x_3) + \bar{u}_\alpha(\bar{x}, -x_3) \quad \text{for } \alpha = 1, 2, \\
 v_3(x) &:= \bar{u}_3(\bar{x}, x_3) - \bar{u}_3(\bar{x}, -x_3).
 \end{aligned}$$

With their help we rewrite problem (40) for  $v = (v_1, v_2, v_3)$  over the half-space as

$$\begin{aligned}
 -\mu\Delta v - (\mu + \lambda)\nabla(\operatorname{div} v) &= 0 && \text{in } \mathbb{R}_+^3, \\
 \sigma_{13}(v) = \sigma_{23}(v) &= 0 && \text{on } \Sigma^+, \\
 v(x) &= o(1) && \text{as } |x| \rightarrow \infty, \\
 v_3(\bar{x}, 0) &= \llbracket \bar{u}_3 \rrbracket(\bar{x}, 0) && \text{for } \bar{x} \in A_c^{n-1}, \\
 (2\mu v_{3,3} + \lambda \operatorname{div}(v))(\bar{x}, 0) &= 2\sigma_{33}(\bar{u})(\bar{x}, 0) && \text{for } \bar{x} \in \mathbb{R}^2 \setminus A_c^{n-1}.
 \end{aligned} \tag{41}$$

A known Papkovitch–Neuber representation of mixed boundary-value problems in half-spaces expresses  $v$  in the form

$$v_\alpha = (\varkappa - 1)U_\alpha - \varkappa x_3 U_{3,\alpha} \quad \text{for } \alpha = 1, 2, \quad v_3 = U_3 - \varkappa x_3 U_{3,3}, \tag{42}$$

where  $\varkappa = \frac{\mu+\lambda}{2\mu+\lambda} > 0$ . The three harmonic potentials  $U = (U_1, U_2, U_3)$  are such that  $\Delta U = 0$  and  $\text{div}(U) = 0$ . Thus, from (41) and (42) we infer that  $U_3$  satisfies the following relations

$$\begin{aligned} \Delta U_3 &= 0 \quad \text{in } \mathbb{R}_+^3, & U_3(x) &= o(1) \quad \text{as } |x| \rightarrow \infty, \\ U_3(\bar{x}, 0) &= \llbracket \bar{u}_3 \rrbracket(\bar{x}, 0) \quad \text{for } \bar{x} \in A_c^{n-1}, \\ U_{3,3}(\bar{x}, 0) &= \frac{1}{\mu\varkappa} \sigma_{33}(\bar{u})(\bar{x}, 0) \quad \text{for } \bar{x} \in \mathbb{R}^2 \setminus A_c^{n-1}. \end{aligned} \tag{43}$$

During the iteration  $n \geq 1$  of the active set in (38), we have  $\llbracket \bar{u}_3 \rrbracket(\bar{x}, 0) \leq 0$ , hence  $U_3(\bar{x}, 0) \leq 0$  for  $\bar{x} \in A_c^{n-1}$  in (43). If  $\sigma_{33}(\bar{u})(\bar{x}, 0) \leq 0$ , then  $U_{3,3}(\bar{x}, 0) \leq 0$  for  $\bar{x} \in \mathbb{R}^2 \setminus A_c^{n-1}$ . The maximum principle applied to the function  $U_3(\bar{x}, x_3)$ , which is harmonic in  $\mathbb{R}_+^3$ , results in the necessary conclusion  $U_3(\bar{x}, 0) \geq 0$  for  $\bar{x} \in \mathbb{R}^2 \setminus A_c^{n-1}$ . Thus,  $\sigma_{33}(\bar{u}) \leq 0$  at  $\mathbb{R}^2 \setminus A_c^{n-1}$  follows that  $\llbracket \bar{u}_3 \rrbracket \geq 0$  at  $\mathbb{R}^2 \setminus A_c^{n-1}$ . The assertion (39) is proved.